New Measurements of Some Double Stars in the Constellation Vulpecula

Zsolt Szamosvari
Hungarian Astronomical Association Double Star Section
H-2500 Esztergom, Hungary.
szamos.photo@gmail.com

Abstract

The purpose of these research is to measure rarely observed double stars in the constellation Vulpecula, especially members of multiple systems. During work, were managed to observe 59 pairs as a primary target and 89 pairs as a secondary target. Were also found 2 new possible binary stars and more new members for seven system. All observed pairs were processed using Harshaw's method and the probability of gravitational bonding was established.

1. Introduction

The Washington Double Star Catalog (WDS) contains many visual double stars that have been rarely observed, leaving few measurements available for further investigation. That is why were chose the re-observation of neglected pairs as the subject of our research. First was selected the constellation Vulpecula, which is in a good position in summer for observations. To select the targets, were used the special search engine of the Stelle Doppie website (Sordiglioni, 2023). Table 1 shows the search criteria. When defining the criteria, also were considered the technical characteristics of the instrument to be used, the T21 telescope of the iTelescope network.

Mag. primary	between 7-11
Δ mag	< 3
Separation	between 5" - 50"
Last observation	< 2015
Number of obs.	between 3-15
Members of system	> 3
Gaia ID	yes

Table 1. Search criteria

The results of filtering, 16 pairs, are shown in Table 2.

Coord	WDS Name	Last	Obs	Pa	Sep	M1	M2	Δ mag
20 32 51 +29 02 35	ARY 27 BC	2015	14	50	35.3	8.32	10.89	2.57
20 22 48 +27 09 09	ARN 50 CD	2015	15	186	25.9	8.85	9.1	0.25
20 18 17 +25 39 15	BU 985 CD	2015	13	67	8.6	10.87	13.6	2.73
19 48 55 +25 49 48	BKO 740 AB	2015	13	38	15.9	10.32	10.75	0.43
21 06 29 +26 55 05	STF 2756 AB	2015	11	48	11.9	10.2	12.3	2.1
21 04 29 +24 57 04	SLE 520 AB	2015	10	346	34.3	9.73	11.62	1.89
20 47 39 +25 18 00	POU 4996 DH	2015	8	127	12	10.78	13.4	2.62
20 46 19 +27 40 47	MLB 712 AB	2015	10	43	8.5	10.49	12	1.51
20 33 04 +28 51 48	ES 507 AB	2015	11	295	7.1	8.78	11.4	2.62
20 30 47 +26 57 35	OPI 25 AC	2015	9	324	27	10.03	12.5	2.47
20 30 11 +26 50 34	LMP 45 AF	2015	10	252	43.7	10.5	13.1	2.6
20 18 38 +28 31 59	HJ 1501 AB	2015	10	355	12.9	10.18	11.1	0.92
19 38 36 +24 54 32	POU 3973 AC	2015	10	230	7.6	10.53	11.5	0.97
19 36 23 +25 03 51	DOO 76 AB	2015	14	145	24.4	8.66	11.3	2.64
19 28 13 +20 12 60	WAL 113 AC	2015	14	327	36.8	10.1	11.47	1.37
19 23 13 +22 09 53	HJ 886 AB	2015	15	45	8.2	10.41	11.4	0.99

Table 2. List of targets

2. Equipment and Methods

The images of the double stars were acquired by the T21 telescope, located in Beryl Junction Utah, USA, at an elevation of 1,570 meters. The CCD camera for T21 is an FLI-PL 6303E with a resolution of 0.96" per pixel, housing a pixel array 3072 by 2078, with a FOV of 32.8 by 49.2 arcminutes. The CCD camera is mounted on a Planewave 17 Corrected Dirk-Kirkham (CDK) OTA, with a focal length of 1,940 mm with an aperture of 431 mm and a focal ratio of f/4.5. Exposure times of 60 s with a luminance filter were taken fir 10 images. Figure 1 shows the instrument (source: iTelescope.net).

For measurements, were used AstroImageJ (Collins et al, 2017) software. The FITS files were calibrated using *astronomy.net key* within the software. At this point, the program shows the images with the correct skyline, and allows for accurate separation and position angle measurement. Were adjusted the brightness and aperture sizes individually to get the best results.

Astrometric data were obtained from GAIA DR3 via the Aladin interactive sky atlas (Bonnarel et al, 2000) and the Simbad database (Wenger et al, 2000). These were stored in a new spreadsheet based on the Rowe-Harshaw Excel spreadsheet (Harshaw, 2018). From the GAIA coordinates of the members, were calculate the position angles and separations for the 2016 epoch (Buchheim, 2008). Were requested historical data of pairs from USNO, which were supplemented with calculated GAIA positions and the new measurements. The detailed analysis of the pairs was performed in the Plot Tool Excel spreadsheet (Harshaw, 2020).

To establish binary probability, were considered several indicators: the *Harshaw Rating* (the distance between two stars and their proper motion, the relationship between total velocity and escape velocity), the relationship between maximum orbital velocity and observed velocity, the limit of the gravitational bond derived from the mass of the primary star, and the limit of the gravitational bond derived from the total masses of the two stars.

The mathematical formulas for calculating total velocity and escape velocity are known from previous works, which I will not describe further. The maximum orbital velocity and observed orbital velocity are more interesting. It was first used by Sinachopoulos and Mouzourakis to establish gravitational bonds in 1992.

Figure 1.: the T21 telescope

To calculate the maximum orbital velocity, the equation "vis viva" is applied:

$$v_{orb\_max} = \sqrt{G(M+m)\left(\frac{2}{s}-\frac{1}{a}\right)} \qquad (1)$$

where M is the primary, m is the mass of the secondary star in $M_\odot$, s is the distance between the two stars in parsec, a is semi-major axis in parsec, G is the gravitational constant.

The observed orbital velocity is calculated according to the formulas (Rica, 2011):

$$\Delta u = \sqrt{\left(\rho\frac{\Delta\theta}{\Delta t}\right)^2 + \left(\frac{\Delta\rho}{\Delta t}\right)^2} \qquad (2)$$

Δu is displacement of the secondary around the primary, ρ is the last separation, $\Delta\Theta$ is difference of the position angle, $\Delta\rho$ is the difference of the separation, Δt is the difference of the time.

$$v_{obs} = 0{,}0474\, d\, \Delta u \qquad (3)$$

where d is the distance of the system from Earth, in parsec. If the v_{obs} is smaller than v_{orb_max}, then a gravitational bond is possible.

The advantage of this calculation over total velocity calculation is that it can be calculated from historical data, whereas in many cases the radial velocity required for total velocity is missing from GAIA's DR3 database.

To calculate gravitational bond limits of stars, were used the following formulas (Rica Romero, 2010):

$$d_{max}AU = 2500(M_A)^{1{,}54} \qquad (4)$$

where d_{max} is the primary limit in AU, M_A is the mass of the primary in $M_\odot$.

$$a_{max} = 1000\left(\frac{M_{tot}}{0{,}185}\right) \quad (5)$$

where a_{max} is the limit of the combined gravitational bond of the two stars, M_{tot} is the sum of the masses of the two stars in $M_\odot$ (Rica Romero, 2010).

The various indicators were weighted. Harshaw Rating gets 90% weight, speeds get 5% weight, gravity limits get 2.5% weight, and Plot tool R2 gets 2.5% weight. That's 100% in total. To evaluate binary probability, Harshaw's limits were used, which are summarized in Table 3 (Harshaw, 2018).

Threshold (%)	Class
>85	Physical
85 - 65	Physical?
65 - 50	Maybe
50 - 35	??
35 - 0	No

Table 3.: Thresholds

3. Data summary

The target 16 pairs are part of 16 multiple systems. Each member of these systems was measured and analyzed including historical data using the Plot tool spreadsheet. In the end, were obtained new measurement results for 59 pairs, which are summarized in Table 5. Were called these systems the primary targets. The findings of their detailed analysis are shown in Table 4 and Figure 2.

Type	Primary	Secondary
Unk	2	4
No	17	17
??	11	13
Maybe	11	13
Y?	8	27
Y	10	15
Sum	**59**	**89**

Table 4.: Summary of targets

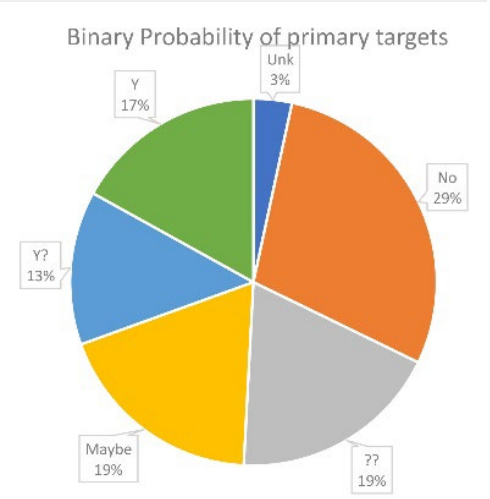

Figure 2.: Distribution of primary targets

It can be concluded that out of 59 pairs, a total of 30%, 18 pairs, turned out to be physical double stars, the rest are of questionable physicality. In many cases, this is due to the low number of observations. Some 22 pairs are questionable, and 17 pairs are surely optical double.

In addition to the primary systems, 89 other binary systems were found by examining the images. These are called secondary targets. The measurement results of the secondary targets are included in Table 6. The results of them detailed analyses are shown in Table 4 and Figure 3.

Among the secondary targets, 89 pairs are members of 42 systems. 47% of these pairs turned out to be physical double stars. This is already a better ratio than in the case of primary targets.

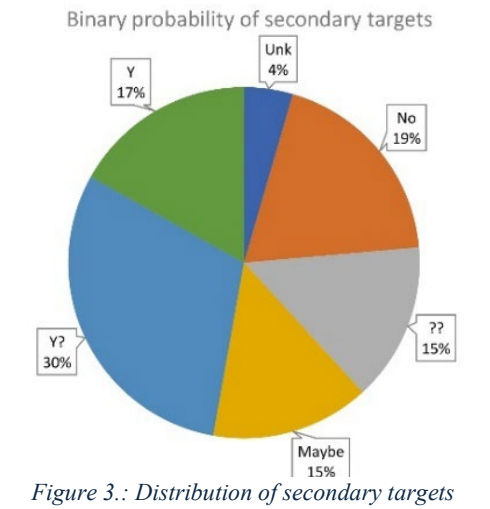

Figure 3.: Distribution of secondary targets

As a function of absolute magnitude and effective temperature, were also plotted the stars on the Hertzsprung-Russel Diagram (HRD). From Figure 4. it can see that the stars do not cover the entire HRD, but part of the main sequence and the giant arm are nicely drawn. Most of the stars are clustered at the base of the main sequence and giant arm. The compaction can be explained by looking at the spectral distribution of stars. Here were include only the spectral classes estimated by the Plot tool, since there are very few spectral types for individual stars found in different catalogs (Figure 5).

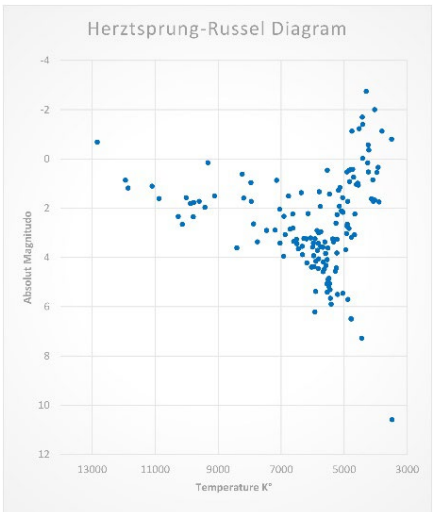

Figure 4.: Observed stars on HRD

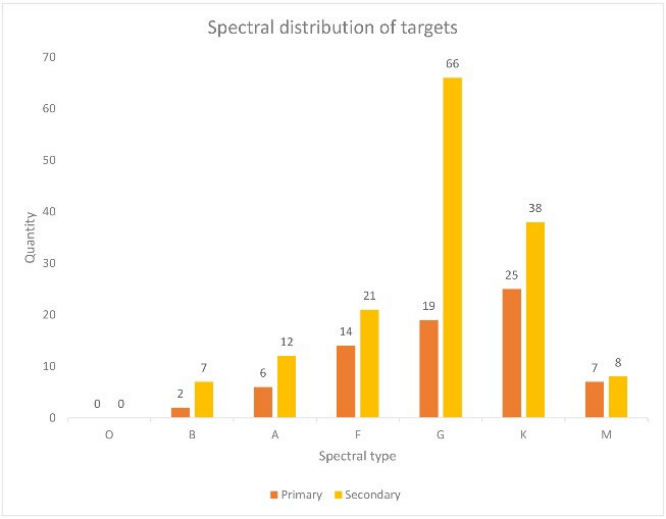

Figure 5.: Spectral type of stars

4. Measurement data

Explanation for the following tables. The *WDS* and *Disc* columns contain double identifiers. The *Comp* column contains component markings. In the *Separation* and *Position Angle* and Δ *mag* columns, the *AVG* columns represent the measurement averages, and the *STD* columns contain the standard errors. The *Date* column shows the date of observation. The *Binary Probability* column shows the probability of physicality. Possible new binary stars are marked *CND* (candidate) in the *Disc* column.

Nº	WDS	Disc	Comp	Separation		Position Angle		Δ mag		Date	Binary Proba-bility	Notes
				AVG	STD	AVG	STD	AVG	STD			
1	20229+2708	ARN50	AC	85.07	0.14	330.62	0.02	0.19	0.01	2023.582	55.22%	1
2	20229+2708	ARN50	AD	65.63	0.1	318.1	0.09	0.42	0.02	2023.582	93.66%	
3	20229+2708	ARN50	CD	25.36	0.13	184.72	0.08	0.23	0.03	2023.582	56.78%	
4	20183+2539	HJ1499	AC	21.6	0.33	353.65	0.77	1.12	0.05	2023.585	76.05%	
5	20183+2539	WAL131	AE	122.68	0.09	151.2	0.03	0.42	0.01	2023.585	72.83%	
6	20183+2539	BU985	CD	8.77	0.18	67.56	1.5	2.9	0.06	2023.585	49.69%	
7	21065+2655	STF2756	AB	11.79	0.04	49.37	0.23	1.82	0.06	2023.59	No Px	2
8	21065+2655	STF2756	AC	75.02	0.03	287.94	0.04	1.18	0.02	2023.59	No Px	2
9	21045+2457	SLE520	AB	34.58	0.05	345.78	0.05	1.72	0.01	2023.599	23.77%	
10	21045+2457	SLE520	AC	43.5	0.04	144.49	0.05	2.23	0.01	2023.599	47.93%	
11	21045+2457	SLE520	BD	17.92	0.01	117.63	0.08	2.12	0.01	2023.599	31.76%	
12	20327+2903	ARY47	AB	128.13	0.03	107.56	0.04	0.04	0	2023.601	45.91%	
13	20327+2903	ARY27	BC	35.35	0.03	49.13	0.08	2.23	0.02	2023.601	23.12%	
14	20327+2903	ARY27	BD	89.93	0.05	178.3	0.01	0.99	0.01	2023.601	62.22%	
15	20331+2852	ES507	AB	7.24	0.19	294.89	1.79	1.52	0.03	2023.601	93.45%	
16	20331+2852	ES507	AC	36.27	0.04	345.85	0.04	0.86	0.01	2023.601	46.44%	
17	20331+2852	ES507	AD	36.9	0.03	223.67	0.06	1.04	0.01	2023.601	16.18%	

18	20331+2852	FMY137	AE	42.74	0.02	101.18	0.05	5.7	0.03	2023.601	50.49%	
19	20331+2852	FMY137	AF	23.14	0.29	176.41	0.21	5.52	0.02	2023.601	15.40%	
20	20331+2852	FMY137	AG	32.69	0.05	299.18	0.08	5.58	0.04	2023.601	41.93%	
21	20331+2852	ES507	DS	16.06	0.03	145.96	0.04	2.79	0.03	2023.601	51.58%	
22	19489+2550	BKO740	AB	15.91	0.03	37.4	0.1	0.46	0	2023.602	47.33%	
23	19489+2550	BKO740	AD	18.83	0.02	92.33	0.15	3.16	0.02	2023.602	61.50%	
24	19489+2550	BKO740	BC	7.93	0.16	263.89	0.32	2.93	0.01	2023.602	72.86%	
25	19489+2550	BKO740	DE	2.79	0.16	314.89	2.25	0.9	0.19	2023.602	55.26%	
26	20478+2519	BUP218	AB	49.65	0.02	36.6	0.03	0.12	0.01	2023.641	49.42%	
27	20478+2519	BUP218	AC	102.87	0.02	98.86	0.01	1.15	0.01	2023.641	8.83%	
28	20478+2519	BUP218	AD	153.76	0.03	252.51	0.02	0.61	0	2023.641	28.08%	
29	20478+2519	DAM514	AF	44.21	0.04	99.46	0.02	1.94	0.02	2023.641	61.54%	
30	20478+2519	WSI49	BE	5.32	0.53	141.1	1.18	3.46	0.15	2023.641	37.68%	
31	20478+2519	POU4996	DH	11.85	0.08	128.27	0.36	2.86	0.02	2023.641	75.98%	
32	20478+2519	BKO856	FG	9.13	0.03	178.83	0.36	0.32	0.01	2023.641	16.70%	
33	20463+2740	MLB712	AB	8.54	0.08	42.3	0.4	2.72	0.06	2023.672	57.53%	
34	20463+2740	MLB712	AC	23.96	0.04	125.47	0.04	0.92	0.05	2023.672	48.52%	
35	20463+2740	BRT3362	CD	6.07	0.22	84.86	0.7	1.72	0.02	2023.672	94.12%	
36	19365+2502	DOO76	AB	24.54	0.07	145.43	0.13	3.07	0.08	2023.624	57.53%	
37	19365+2502	DOO76	AC	43.39	0.09	167.55	0.06	1.47	0.05	2023.624	86.13%	
38	19365+2502	FYM82	AE	15.26	0.27	316.57	0.16	4.54	0.05	2023.624	31.34%	
39	19365+2502	FYM82	AF	21.47	0.06	201.59	0.15	4.76	0.11	2023.624	34.56%	
40	19365+2502	DOO76	CD	2.23	0.18	259.61	3.05	0.34	0.12	2023.624	91.94%	
41	19386+2455	POU3975	AB	4.35	0.34	104.34	1.51	2.8	0.17	2023.624	34.31%	
42	19386+2455	POU3973	AC	7.52	0.11	229.61	0.49	0.86	0.03	2023.624	54.05%	
43	19386+2455	POU3974	AD	21.37	0.05	225.69	0.12	1.53	0.02	2023.624	25.17%	
44	19232+2209	HJ886	AB	8.2	0.04	45.34	0.23	0.84	0.02	2023.627	91.40%	
45	19232+2209	SLE939	AC	31.8	0.08	199.52	0.13	0.39	0.02	2023.627	90.68%	
46	19232+2209	SLE939	AD	57.17	0.08	144.65	0.06	0.31	0.02	2023.627	89.63%	
47	19282+2013	STF3132	AB	7.56	0.12	38.64	1.02	0.73	0.05	2023.627	92.98%	
48	19282+2013	WAL113	AC	36.26	0.14	325.78	0.3	1.61	0.04	2023.627	45.83%	
49	19282+2013	WAL113	AD	56.28	0.13	307.35	0.23	1.85	0.03	2023.627	23.02%	
50	20186+2833	HJ1501	AB	12.86	0.04	354.04	0.11	0.99	0.02	2023.643	19.00%	
51	20186+2833	HJ1501	AC	57.18	0.04	349.2	0.03	1.09	0.01	2023.643	74.52%	
52	20186+2833	HJ1501	CD	20.35	0.02	12.31	0.07	1.61	0.03	2023.643	18.84%	
53	20302+2651	BUP213	AC	9.91	0.04	324.28	0.27	2.92	0.02	2023.61	84.16%	3
54	20302+2651	BUP213	AD	92.21	0.05	281.92	0.03	1.06	0.02	2023.61	83.87%	
55	20302+2651	BUP213	AE	1342.03	0.32	92.97	0.01	0.38	0.02	2023.61	82.98%	
56	20302+2651	LMP45	AF	42.37	0.02	253.14	0.03	3.42	0.02	2023.61	87.48%	
57	20307+2657	OPI25	AB	14.19	0.04	29.85	0.15	3.71	0.02	2023.643	46.47%	
58	20307+2657	OPI25	AC	27.12	0.02	325.07	0.09	2.68	0.01	2023.643	23.70%	
59	20307+2657	OPI25	AD	103.88	0.06	357.33	0.03	1.86	0.02	2023.643	26.14%	

Table 5.: Measurements of primary targets

Notes:

1. 20229+2708 AB I couldn't measure it because it didn't separate.
2. 21065+2655 there isn’t parallax of the primary.
3. 20302+2651 I couldn't measure it because it didn't separate.

Nº	WDS	Disc	Comp	Separation		Position Angle		Δ mag		Date	Binary Probability	Notes
				AVG	STD	AVG	STD	AVG	STD			
1	17503-2621	DAM371	AB	6.18	0.02	58.77	0.34	0.22	0.01	2023.578	92.15%	
2	17503-2620	HJ4986	AB	10.58	0.02	225.67	0.23	2.03	0.05	2023.578	92.90%	
3	17503-2620	HJ4986	AC	23.33	0.03	3.53	0.07	4.33	0.05	2023.578	28.32%	
4	17503-2620	HJ4986	AD	27.18	0.03	58.96	0.16	3.24	0.06	2023.578	13.84%	
5	19478+2615	BRT201	AB	2.92	0.16	359.89	0.76	0.02	0.03	2023.589	33.92%	
6	19478+2612	SCA200	AB	2.90	0.20	138.66	2.08	0.02	0.03	2023.589	33.29%	
7		CND41	AB	43.64	0.05	42.79	0.05	0.73	0.02	2023.589	48.35%	1
8		CND41	AC	41.38	0.02	91.98	0.10	3.43	0.04	2023.589	80.23%	1
9		CND41	BC	35.45	0.02	160.71	0.04	2.70	0.05	2023.589	76.88%	1
10		CND42	AB	38.08	0.02	146.81	0.02	0.59	0.03	2023.589	68.85%	2
11	21030+2457	BKO482	AB	5.97	0.08	358.72	0.41	1.06	0.02	2023.599	27.80%	
12	21033+2454	BKO483	AB	8.42	0.10	71.89	0.28	0.14	0.01	2023.599	80.61%	
13	21050+2458	GRV411	AB	45.84	0.04	348.66	0.04	0.68	0.00	2023.599	80.79%	
14	21030+2458	POU5110	AB	12.43	0.03	146.01	0.17	1.40	0.01	2023.599	21.48%	
15	21032+2453	POU5114	AB	2.29	0.12	338.06	2.20	0.36	0.03	2023.599	73.66%	
16	21042+2449	POU5126	AB	20.20	0.07	141.79	0.26	0.37	0.01	2023.599	77.47%	
17	21046+2502	POU5133	AB	6.20	0.03	311.30	0.21	0.65	0.01	2023.599	74.84%	
18	21047+2504	POU5134	AB	14.07	0.03	201.27	0.09	0.30	0.00	2023.599	41.07%	
19	21047+2446	POU5135	AB	19.93	0.06	178.14	0.13	0.48	0.02	2023.599	76.91%	
20	21047+2446	CND43	AC	3.92	0.17	15.57	0.69	0.24	0.02	2023.599	52.86%	3
21	21051+2454	POU5141	AB	15.54	0.02	346.10	0.13	1.00	0.01	2023.599	19.75%	
22	21051+2454	POU5142	AC	17.72	0.16	327.79	0.85	1.45	0.05	2023.599	18.53%	
23	21051+2454	POU5142	BC	6.03	0.10	268.93	0.80	0.55	0.01	2023.599	92.01%	
24	21053+2444	POU5144	AB	16.53	0.04	331.48	0.16	1.52	0.01	2023.599	40.20%	
25	21053+2447	POU5145	AB	9.88	0.02	150.19	0.24	0.22	0.01	2023.599	18.17%	
26	21056+2510	POU5149	AB	16.64	0.03	275.40	0.10	0.60	0.01	2023.599	43.74%	
27	21059+2458	POU5151	AB	12.43	0.05	27.88	0.14	1.00	0.00	2023.599	75.98%	
28	21060+2451	POU5153	AB	5.30	0.39	20.98	2.10	1.94	0.08	2023.599	55.92%	
29	21063+2457	POU5156	AB	5.40	0.43	280.43	1.54	2.18	0.13	2023.599	42.65%	
30	21063+2449	POU5157	AB	4.51	0.18	87.53	1.24	1.00	0.03	2023.599	68.35%	
31	20312+2855	ES506	AB	4.88	0.28	302.66	1.62	0.70	0.13	2023.601	91.72%	
32	20320+2915	GRV349	AB	33.18	0.02	42.49	0.02	2.38	0.01	2023.601	43.84%	
33	20346+2914	J565	AB	6.95	0.06	47.51	0.38	1.55	0.03	2023.601	58.19%	
34	20346+2914	J565	AC	16.31	0.27	86.48	0.21	3.86	0.02	2023.601	25.62%	
35	17069+2254	KUI123	AB	21.73	0.03	298.00	0.11	1.32	0.01	2023.602	41.32%	
36	20487+2507	BKO862	AB	7.93	0.53	57.88	3.34	1.37	0.27	2023.641	88.98%	
37	20490+2504	BKO864	AB	9.21	0.35	314.77	1.92	3.65	0.07	2023.641	26.86%	
38	20491+2509	BKO865	AB	9.02	0.12	101.16	0.71	0.41	0.10	2023.641	78.07%	
39	20500+2508	BKO874	AB	12.48	0.10	254.24	0.65	0.89	0.08	2023.641	28.76%	
40	20462+2513	POU4972	AB	13.80	0.14	279.76	0.22	0.41	0.03	2023.641	64.06%	
41	20462+2526	POU4974	AB	17.25	0.08	106.71	0.11	1.53	0.03	2023.641	64.18%	
42	20465+2506	POU4980	AB	7.37	0.07	145.44	0.94	0.49	0.03	2023.641	28.39%	
43	20465+2506	POU4979	AC	12.95	0.10	105.51	0.49	0.52	0.06	2023.641	58.82%	
44	20480+2504	POU5001	AB	7.77	0.08	197.65	0.71	0.70	0.03	2023.641	64.46%	
45	20482+2508	POU5003	AB	14.58	0.08	208.03	0.26	3.17	0.06	2023.641	30.32%	

46	20483+2515	POU5004	AB	14.93	0.03	321.43	0.19	0.25	0.01	2023.641	79.51%	
47	20492+2504	POU5020	AB	4.26	0.31	65.85	2.08	0.78	0.09	2023.641	45.36%	
48	20492+2510	POU5021	AB	5.71	0.10	354.06	0.63	1.22	0.05	2023.641	88.98%	
49	20299+2624	S750	AB	68.46	0.08	320.32	0.04	0.15	0.00	2023.61	61.65%	
50	20310+2629	STF2692	AB	10.25	0.35	164.87	2.22	1.41	0.15	2023.61	No Px	
51	20310+2629	STF2692	AC	25.81	0.02	300.79	0.08	0.55	0.01	2023.61	92.66%	
52	20310+2629	FMY62	AD	27.97	0.04	57.45	0.05	5.58	0.02	2023.61	11.30%	
53	19348+2517	J1239	AB	4.23	0.36	247.41	2.08	1.94	0.09	2023.624	94.21%	
54	19350+2518	POU3933	AB	15.75	0.02	283.42	0.14	0.48	0.03	2023.624	86.31%	
55	19352+2501	POU3940	AB	9.75	0.06	26.61	0.42	0.16	0.03	2023.624	72.08%	
56	19365+2500	STF2548	AB	9.31	0.05	99.03	0.33	0.66	0.07	2023.624	53.37%	
57	19393+2451	BKO427	AB	8.85	0.02	312.62	0.15	0.53	0.01	2023.624	36.10%	
58	19399+2447	BKO430	AB	9.18	0.01	322.36	0.08	0.12	0.01	2023.624	71.06%	
59	19399+2447	CND44	AC	4.16	0.05	274.06	2.09	2.87	0.04	2023.624	80.60%	4
60	19399+2447	CND44	AD	14.90	0.02	240.95	0.12	1.51	0.01	2023.624	71.58%	4
61	19399+2447	CND44	AE	16.47	0.03	57.30	0.16	2.70	0.03	2023.624	77.41%	4
62	19369+2447	POU3962	AB	13.92	0.02	266.67	0.03	0.97	0.01	2023.624	62.50%	
63	19387+2444	POU3978	AB	13.72	0.03	229.60	0.21	1.17	0.01	2023.624	45.00%	
64	19387+2444	CND45	AC	6.02	0.02	339.05	0.20	2.67	0.02	2023.624	70.21%	5
65	19388+2444	POU3980	AB	2.89	0.04	260.95	3.32	0.32	0.04	2023.624	22.38%	
66	19392+2508	POU3983	AB	5.87	0.24	211.84	1.09	2.98	0.04	2023.624	93.68%	
67	19394+2504	POU3989	AB	15.66	0.05	177.46	0.09	3.71	0.03	2023.624	43.21%	
68	19397+2450	POU3992	AB	11.15	0.05	229.44	0.25	0.38	0.00	2023.624	46.54%	
69	19397+2450	BKO428	AC	3.98	0.20	266.42	0.79	2.00	0.04	2023.624	90.48%	
70	19397+2450	BKO428	BD	4.14	0.06	161.25	2.77	2.15	0.03	2023.624	82.90%	
71	19397+2454	POU3993	AB	12.54	0.05	110.13	0.13	2.36	0.03	2023.624	69.33%	
72	19398+2449	POU3995	AB	14.68	0.04	133.83	0.20	3.44	0.02	2023.624	No Px	
73	19398+2449	BKO429	AC	12.37	0.05	33.14	0.22	3.85	0.02	2023.624	No Px	
74	19399+2455	POU3998	AB	16.00	0.03	313.43	0.10	0.31	0.01	2023.624	73.62%	
75	19399+2455	CND46	AC	2.69	0.10	20.13	3.76	1.59	0.05	2023.624	64.30%	6
76	19399+2438	POU3999	AB	18.74	0.01	275.35	0.05	1.25	0.01	2023.624	80.69%	
77	19400+2452	POU4001	AB	7.74	0.02	321.58	0.15	0.52	0.01	2023.624	55.73%	
78	19400+2450	POU4002	AB	12.76	0.03	337.94	0.11	0.78	0.01	2023.624	57.81%	
79	19234+2215	SLE940	AB	2.82	0.32	205.68	2.73	0.48	0.06	2023.627	94.98%	
80	19247+2208	SLE942	AB	14.54	0.03	335.58	0.05	0.41	0.01	2023.627	35.74%	
81	19248+2159	SLE943	AB	20.74	0.02	266.74	0.07	0.17	0.01	2023.627	No Px	
82	19247+2212	TOK332	AB	256.55	0.16	41.88	0.02	6.25	0.03	2023.627	93.82%	
83	19293+2010	AZC106	AB	33.83	0.04	139.92	0.12	5.86	0.04	2023.627	93.55%	
84	19284+2019	STF2530	AB	5.07	0.22	152.96	1.84	0.08	0.01	2023.627	97.40%	
85	20291+2700	DOO86	AB	18.73	0.01	210.19	0.04	0.95	0.00	2023.643	69.69%	
86	20291+2700	CND47	AC	21.62	0.03	109.00	0.09	3.92	0.02	2023.643	70.70%	7
87	20291+2700	CND47	AD	32.57	0.03	51.59	0.04	3.22	0.01	2023.643	82.63%	7
88	20293+2700	DOO93	AC	27.39	0.02	226.57	0.03	1.48	0.01	2023.643	73.13%	
89	20324+2703	DAM328	AB	11.81	0.26	76.06	0.30	3.93	0.04	2023.652	32.78%	

Table 6.: Measurements of secondary targets

Notes:

The explanation for the following plots. The *SZM* notation is my measurement (my own name code in WDS), the red arrow is the predicted resultant motion vector, the green arrow is the measured motion vector. The dashed arrow is a trend line.

1. CND41: HD 338993, new possible triple system at coordinates: $19^h48^m19.45^s$ +26°23'02.25"

The astrometric data for the new triple system are presented in Table 8. Its measurement results can be seen in rows 7-9 of Table 6. Plots in Figure 7.

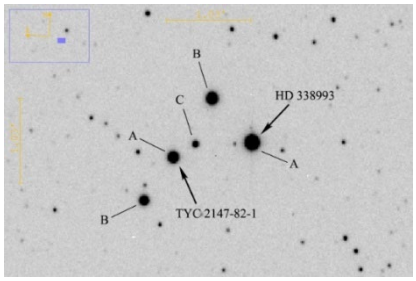

Figure 6.: Two new possible systems, CND 41 and CND 42

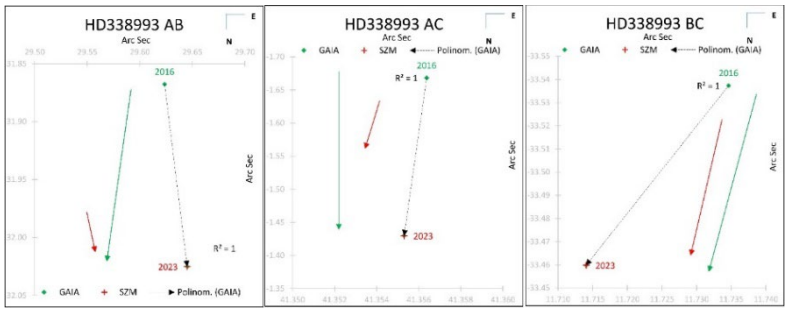

Figure 7.: Plots of new triple system

Comp	Simbad ID	Gaia ID	PM RA	PM Dec	Px	G mag	Rad(☉)	Mass(☉)	Lum(☉)	Spect
A	HD338993	2027782604544202368	-2.54	-5.73	1.29	9.88	5.97	2.90	58.39	A0
B	TYC 2147-138-1	2027782707624110720	2.40	-4.67	1.96	10.78	3.62	1.82	10.98	K
C	No ID	2027782707623403648	0.42	3.96	1.56	13.61	1.22	1.06	1.27	K

Table 8.: Astrometric data of CND41

3. CND42: TYC 2147-82-1, new possible double stars at coordinates: $19^h48^m19.45^s$ +26°23'02.25".

See the Figure 6. The astrometric data for the new double is presented in Table 9. Its measurement results can be seen in row 10 of Table 6. Plot in Figure 8.

Since the two new systems are close to each other, we wondered if they could form a system, but the analysis did not show a positive result. So, they were considered two separate systems.

Comp	Simbad ID	Gaia ID	PM RA	PM Dec	Px	G mag	Rad(☉)	Mass(☉)	Lum(☉)	Spect
A	TYC 2147-82-1	2027781951709153152	-27.78	-22.83	4.02	11.28	1.29	1.13	1.62	G
B	TYC 2147-116-1	2027781882994843136	-17.36	23.75	3.21	11.90	1.23	1.44	1.44	G

Table 9.: Astrometric data of CND42

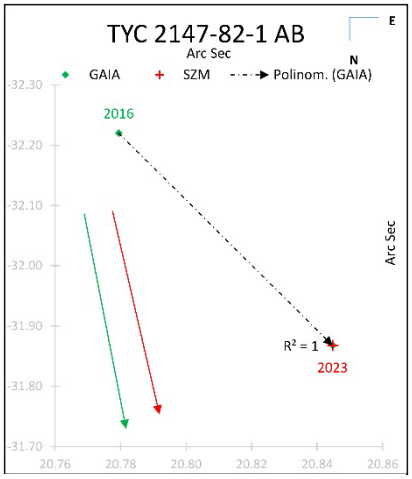

Figure 8.: Plot of CND42

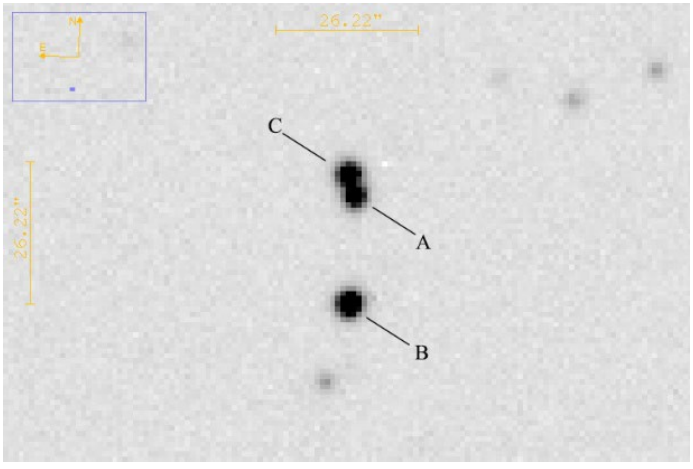

Figure 9.: 21047+2446 (POU5135)

3. CND43: New member of the 21047+2446 (POU5135). See the Figure 9.

The new possible C member appears close to the primary. The analysis showed that there was a 52.86% possibility of physicality. Its measurement result is shown in row 20 of table 6. The astrometric data of members A and C are summarized in Table 10, Figure 10 shows the plots of the system. So, it may be more of a triple system.

Comp	Simbad ID	Gaia ID	PM RA	PM Dec	Px	G mag	Rad(☉)	Mass(☉)	Lum(☉)	Spect
A	No ID	1841192217111877248	5.63	-2.72	0.94	14.64	1.20	1.08	1.37	G
C	No ID	1841192217111877632	-18.69	-15.38	1.57	14.30	0.82	0.90	0.66	G

Table 10.: Astrometric data of 21047+2446 AC

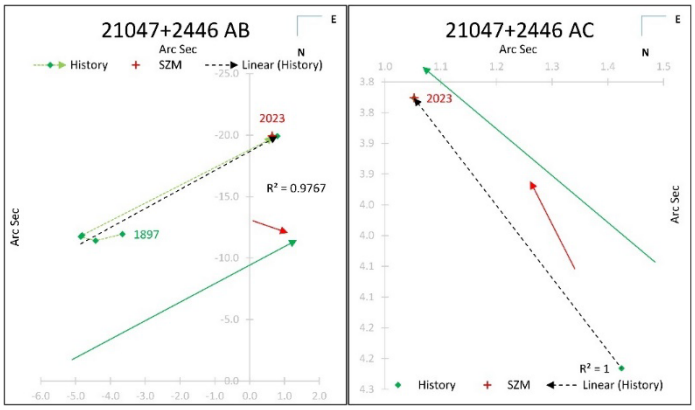

Figure 10.: Plots of 21047+2446 (POU5135)

4. CND44: New members of the 19399+2447 (BKO430). See the Figure 11.

When measuring the system, were noticed the nearby stars, and looked at their Gaia data. Analysis showed that this is a system of five stars. Astrometric data of stars are shown in Table 11, plots are shown in Figure 12. Its measurement results in rows 59-61 of Table 6. The T_{eff} value of star B is missing.

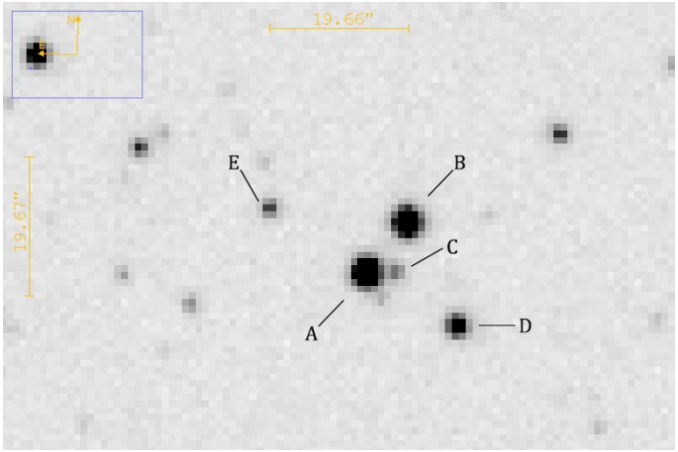

Figure 11.: New quinary system of 19399+2447 (BKO430)

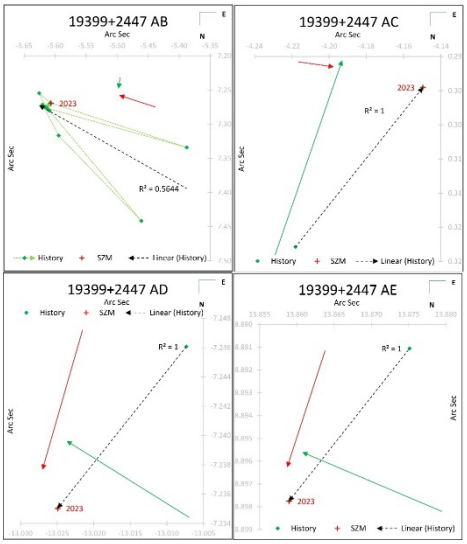

Figure 12.: Plot of 19399+2447 (BKO 430)

Comp	Simbad ID	Gaia ID	PM RA	PM Dec	Px	G mag	Rad(☉)	Mass(☉)	Lum(☉)	Spect
A	No ID	2021196289405496832	-1,28	-4.42	0.38	13.03	6.67	2.55	37.23	K
B	No ID	2021199244342997888	-1.97	-6.49	0.39	13.53	?	2.56	37.61	?
C	No ID	2021196289405497472	-1.43	-5.48	0.33	16.22	1.68	1.26	2.55	G
D	No ID	2021194811936748032	-1.90	-6.53	0.30	14.94	2.37	1.78	10.00	B
E	No ID	2021196289405495680	-1.93	-6.47	0.33	16.05	1.46	1.33	3.09	A

Table 11.: Astrometric data of 19399+2447 (BKO460)

5. CND45: New member of the 19387+2444 (POU3978), see Figure 13.

While measuring the system, were noticed the fainter star next to the primary. A detailed analysis using GAIA data showed the possibility of a physical relationship between star A and star C. Astrometric data of stars are shown in Table 12, plots are shown Figure 14. The measurement data are shown in row 64 of Table 6.

Comp	Simbad ID	Gaia ID	PM RA	PM Dec	Px	G mag	Rad(☉)	Mass(☉)	Lum(☉)	Spect
A	No ID	2021238891137062016	-1.27	-2.93	0.41	14.12	3.66	1.83	11.67	G
C	No ID	2021239101642812416	-2.55	-7.76	0.47	16.71	0.91	0.95	0.80	G

Table 12.: Astrometric data of 19387+2444 AC

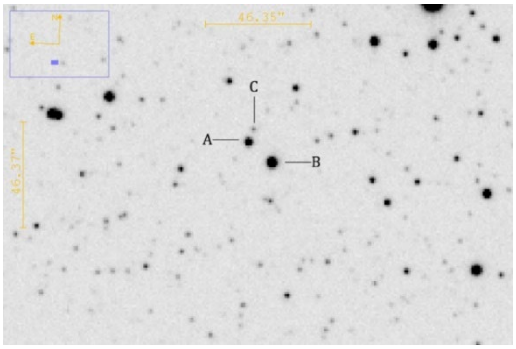

Figure 13.: The 19387+2444 (POU3978) system

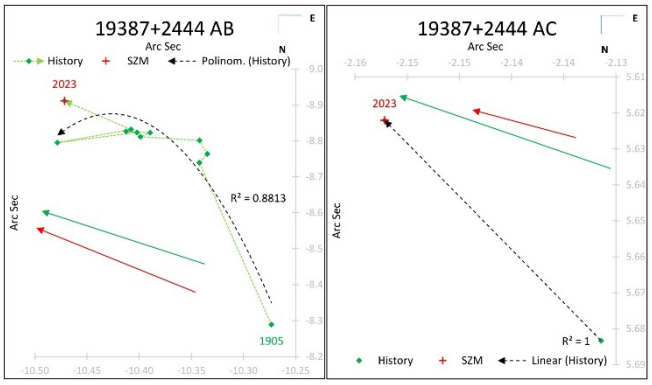

Figure 14.: Plots of 19387+2444 (POU3978)

6. CND46: New member of the 19399+2455 (POU3998). See Figure 15.

In the image, next to the primary, another star was closely visible. Detailed analysis revealed a possible physical relationship between the two stars. Astrometric data are shown in Table 13, plots are shown in Figure 16. The results of measurements are presented in row 75 of Table 6. Unfortunately, the DR3 database missing the T_{eff} value for stars A and C.

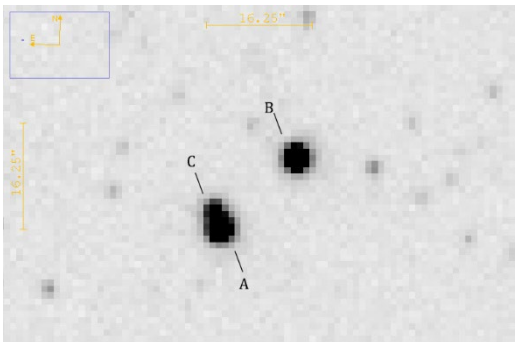

Figure 15.: The 19399+2455 (POU3998) system

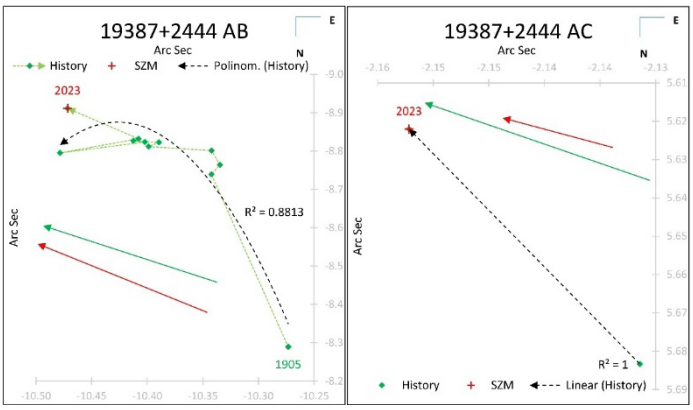

Figure 16.: Plots of 13399+2455 (POU3998)

Comp	Simbad ID	Gaia ID	PM RA	PM Dec	Px	G mag	Rad(☉)	Mass(☉)	Lum(☉)	Spect
A	UCAC4 575-095440	2021201099769213952	-0.11	-1.01	0.63	13.19	?	1.82	11.38	?
C	No ID	2021201099722583552	0.07	-1.33	0.45	15.25	?	1.36	3.43	?

Table 13.: Astrometric data of 19399+2455 AC

7. CND47: Two new members of the 20291+2700 (DOO86). See the Figure 17.

During the measurement, were looked at the data of the stars next to the double in the DR3 database. Were found that C and D stars may have a physical relationship with the primary. Astrometric data are shown in Table 14, plots in Figure 18. The measurement results are shown in rows 86 and 87 of Table 6.

Comp	Simbad ID	Gaia ID	PM RA	PM Dec	Px	G mag	Rad(☉)	Mass(☉)	Lum(☉)	Spect
A	TYC 2164-550-1	1856917363707093376	3.17	-4.37	0.56	12.21	5.10	2.52	35.79	A
C	No ID	1856905612676566272	-4.96	-14.23	0.49	15.98	1.27	1.10	1.46	G
D	No ID	1856917363707090560	0.51	-6.81	0.54	15.28	1.37	1.23	2.26	F

Table 14 Astrometric data of 20291+2700 (DOO86)

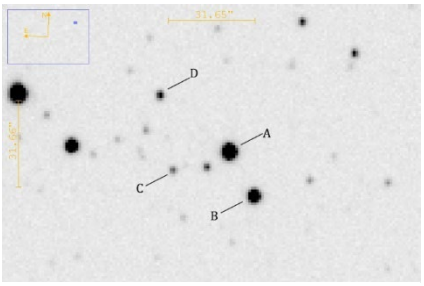

Figure 17.: The 20291+2700 (DOO86) system

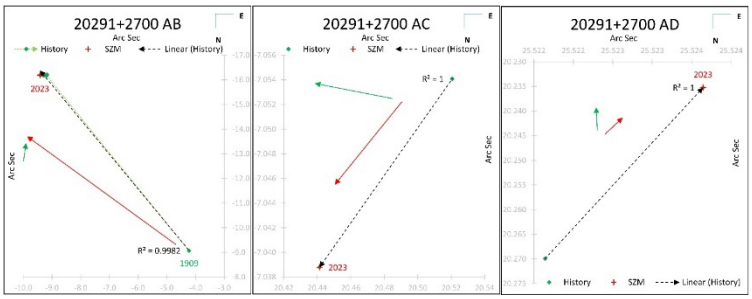

Figure 18.: Plots of 20291+2700 (DOO86)

5. Acknowledgements

Thanks Rachel Matson of the USNO for providing the historical data for this work. I also acknowledge that this work uses the Washington Double Star Catalog maintained at the US Naval Observatory, the SIMBAD database, and the ALADIN sky atlas. This work also used data from the European Space Agency (ESA) Gaia mission (https://www.cosmos.esa.int/gaia) processed by the Gaia Data Processing and Analysis Consortium (https://www.cosmos.esa.int/web/gaia/dpac/consortium). The financing of DPAC was provided by national institutions, especially those participating in the Gaia Multilateral Agreement. Thanks to Richard Harshaw for the Plot tool.

6. References

- Buchheim R. K., "CCD Double-Star Measurements at Altamira Observatory in 2007", JDSO, Vol 4, No. 1, 27-31. Winter 2008.
- Bonnarel, F. et al., "The ALADIN interactive sky atlas. A reference tool for identification of astronomical sources", Astronomy and Astrophysics Supplement, v.143, p.33-40. April 2000.
- Collins, K. A., Kielkopf, J. F., Stassun, K. G., and Hessman, F. V. "AstroImageJ: Image Processing and Photometric Extraction for Ultra-Precise Astronomical Light Curves", Astronomical Journal, 153(77). February 2017.
- Harshaw, R., "Gaia DR2 and the Washington Double Star Catalog: A tale of two databases", JDSO, Vol. 14 No. 4. Page 734-740. October 1, 2018.
- Harshaw, R., "Using Plot Tool 3.19 to Generate Graphical Representations of the Historical Measurement Data", JDSO, Vol. 16 No. 4. Page 386-400. September 1, 2020.

- Rica, F. M., “Determining the Nature of a Double Star: The Law of Conservation of Energy and the Orbital Velocity”, JDSO, Vol. 7, No. 4; 254-259. October 1. 2011.
- Francisco Rica Romero, “Criteria to Determine the Nature of Double Stars: the Stellar Masses”, JDSO. Vol. 6, No. 2; 156-159. April 1. 2010.
- Sinachopoulos&Mouzourakis, “Searching for Optical Visual Double Stars”, Complementary Approaches to Double and Multiple Star Research, IAU Colloquium 135., ASP Conference Series, Vol. 32, 1992 Harold A. McAllister and William I. Hartkopf (eds).
- Gianluca Sordiglioni's (SDG) StelleDoppie: https://www.stelledoppie.it/
- The Washington Double Star Catalog, 2023: http://www.usno.navy.mil/ USNO/astrometry/optical-IR-prod/wds/WDS.
- Wenger, M. et al., “The SIMBAD astronomical database. The CDS reference database for astronomical objects”, Astronomy and Astrophysics Supplement, v.143, p.9-22. April 2000.